

FIELD QUALITY OF MQXFB QUADRUPOLES FOR HL-LHC*

M. Bonora-Tam[†], G. Deferne, G. Dima, L. Fiscarelli, S. Izquierdo Bermudez,
M. Pentella, C. Petrone, CERN, Meyrin, Switzerland

Abstract

This paper presents the main results of the magnetic measurements performed on the Nb₃Sn MQXFB quadrupole magnets for the High Luminosity LHC (HL-LHC) upgrade at both room and cryogenic temperature. The measurement program, carried out during the different stages of the magnet assembly and by using different instruments such as rotating-coil and stretched-wire systems, allows an early identification of the field errors and a comprehensive characterization of the field quality. A fine tuning of the low-order multipoles is achieved by magnetic shims using iron inserts, which provides a means for improving the field quality of some magnets. The transfer function, the field harmonics, and the effects of superconductor magnetization and iron saturation are reported. In addition, a warm-to-cold extrapolation method is developed for the prediction of the integrated gradient at 1.9 K and nominal current, with a target accuracy of 5×10^{-4} , allowing an appropriate sorting of the magnets at an early stage and before the final cold test. In conclusion, all the MQXFB magnets tested so far meet the field-quality requirements for the HL-LHC, and the adopted measurement and correction strategy has proven to be effective for the series production.

INTRODUCTION

The high luminosity upgrade for the LHC (HL-LHC) foresees the replacement of the inner triplet quadrupole magnets in the main experimental insertions housing the ATLAS and CMS experiments, with wider bore, stronger focusing quadrupoles [1]. The new magnets are based on Nb₃Sn cables, and operate at a nominal current of 16.23 kA, corresponding to a gradient of 132.2 T m^{-1} and peak fields of 11.3 T. Including spares, a total of 30 magnets will be produced, in two different length configurations: MQXFA (4.3 m, 20 in total), and MQXFB [2] (7.3 m, 10 in total). The MQXFA will be assembled in the Q1/Q3 cryo-assemblies (2 magnets per assembly), while the MQXFB will be combined with the MCBXFB dipole orbit corrector, see Fig. 1, with two such assemblies (Q2a/Q2b) installed per side of each interaction point. The main design parameters of the MQXFB quadrupoles [3] are reported in Table 1.

A dedicated magnetic measurement program has been implemented for the different stages of magnet assembly with a final test at 1.9 K (cold) [4]. Measurements at ambient temperature (warm) provide early information on geometric field errors, while measurements at cold, and up to nominal current, allow the characterization of all relevant field contri-

butions, including effects of superconductor magnetization and iron saturation.

This paper summarizes the results obtained on the MQXFB series magnets, with emphasis on the transfer function, field harmonics, magnetic shimming, and warm-to-cold extrapolation of the integrated gradient.

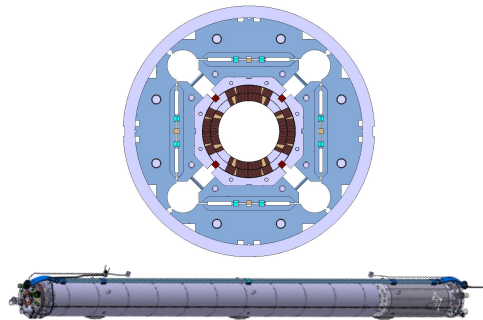


Figure 1: The cross-section of the MQXFB quadrupole (top), and the Q2 cryo-assembly (bottom), integrating the MQXFB quadrupole magnet (left) and the MCBXFB dipole orbit corrector (right).

Table 1: Main Design Parameters of the MQXFB

Parameter	Unit	Value
Aperture diameter	mm	150
Operational temperature	K	1.9
Nominal current I_{nom}	A	16230
Nominal gradient	Tm^{-1}	132.2
Integrated nominal gradient	T	948.1
Magnetic length	m	7.17

MAGNETIC MEASUREMENT STRATEGY

Ambient temperature measurements are carried out at low current (10 A) during several stages of the assembly, including after coil-pack assembly, centering, loading, pre-alignment during cold-mass assembly, and final alignment with respect to reference points.

At 1.9 K, the magnets are measured up to the nominal current of 16.23 kA. The powering program includes stair-step cycles, machine cycles, and variable ramp-rate cycles, optimized to characterize the field within the available test time. In particular, the machine cycles emulate the main features of the operational powering profiles such as the reset current, the injection plateau, the acceleration ramp, and the flattop plateau at nominal current.

Instrumentation includes rotating coils for field harmonics both at warm (rotating coil scanner [5]) and cold (chain of rotating coil shafts [6]), and a stretched-wire system [7, 8] for the transfer function measurement and magnetic axis alignment at warm and cold.

* Work supported by the HL-LHC project

[†] matthias.bonora@cern.ch

MEASUREMENT RESULTS

The magnetic measurements cover the MQXFB series magnets available for HL-LHC installation. At the time of this analysis, MQXFB03 to MQXFB10 were fully completed including their final test at cold, except for MQXFB09 that required a repair. All units required for installation, including the two spares, have been measured at ambient temperature.

Transfer Function

Table 2: Transfer Function of the MQXFB Magnets

Magnet	TF warm [T kA^{-1}]	TF cold [T kA^{-1}]
MQXFB03	63.458	58.571
MQXFB04	63.426	58.654
MQXFB05	63.434	58.700
MQXFB06	63.396	58.523
MQXFB07	63.444	58.563
MQXFB08	63.470	58.594
MQXFB10	63.390	58.487
MQXFB11	63.405	–
MQXFB12	63.441	–
MQXFB09b	63.600	–
Average	63.429	58.585
Range (units)	13	36

The measured transfer function (TF), defined as the integrated gradient normalized to the excitation current is summarized in Table 2 for ambient temperature measurements (warm) and at 1.9 K (cold). Figure 2 shows the transfer functions of all magnets already tested at cold. The average integrated gradient at nominal current is 950.83 T and the magnet-to-magnet spread is in the range of 36 units. Magnet MQXFB09, that required the replacement of one coil after a thermal cycle at 1.9 K, shows a slightly larger TF at warm and is not considered for the estimation of average and range. Magnetic shimming also affects the main field, with a maximum contribution of about 2.0‰ at nominal current when four blades are used.

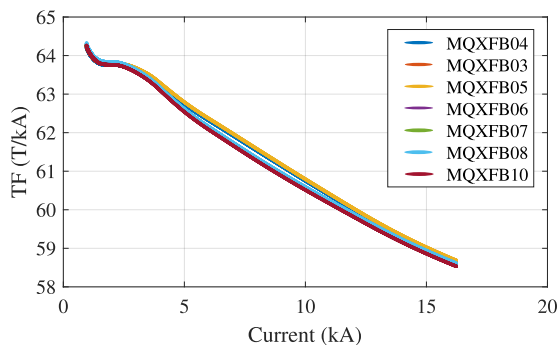


Figure 2: Transfer function as a function of current for the MQXFB magnets already tested at cold.

Field Harmonics and Shimming

The field quality is described by the multipole expansion of the magnetic field at a reference radius of 50 mm and the

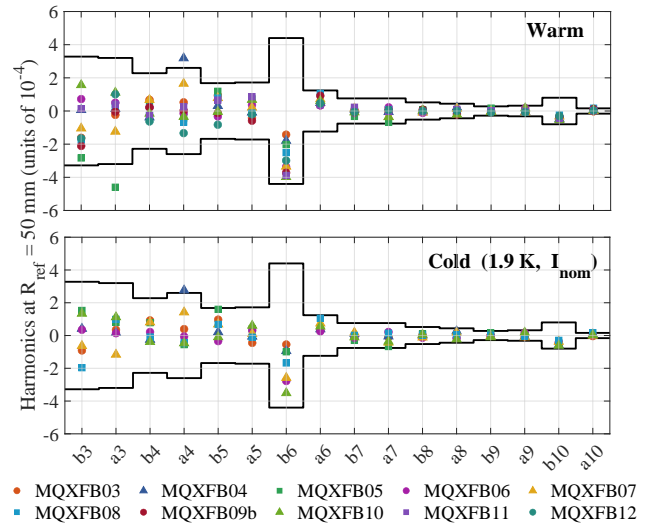


Figure 3: Measured field harmonics at ambient temperature (top) and at 1.9 K and nominal current (bottom). b_3 and a_3 of magnet B05 and a_4 of magnet B04 are corrected by applying magnetic shims. The solid lines refer to the target field quality for nominal HL-LHC optics.

harmonics are expressed in units of 10^{-4} of the main field component. The measured harmonics at ambient temperature and at 1.9 K are within the expected range, see Fig. 3.

Low-order multipoles can be corrected by magnetic shimming. The correction is obtained by inserting iron blades in the bladder slots [9]. The position of the blades is selected using the results of ambient-temperature magnetic measurements and numerical calculations of the expected correction at nominal Current, as shown in Table 3. The effect of the shims is visible in cold conditions, when iron saturation becomes relevant.

Table 3: Computed Magnetic Corrections at I_{nom}

MQXFB04			MQXFB05		
n	Δb_n	Δa_n	n	Δb_n	Δa_n
3	0.00	0.00	3	3.58	3.58
4	0.00	-1.05	4	0.00	0.00
5	0.00	0.00	5	0.33	0.33

This correction strategy has been applied to two series magnets, see Table 3, and has been effective in reducing the selected low-order multipoles. In addition, a systematic b_6 component was corrected by modifying the coil cross-section after the test of the first prototype.

The current dependence of the harmonics shows the expected behavior due to superconductor magnetization at low current and iron saturation at high current. In particular, the allowed b_6 component exhibits a strong variation during the current ramp, as shown in Fig. 4. The effects of the shimming of MQXFB05 are visible in Fig. 5, where the initial high b_3 and a_3 measured at warm are corrected at nominal current at cold.

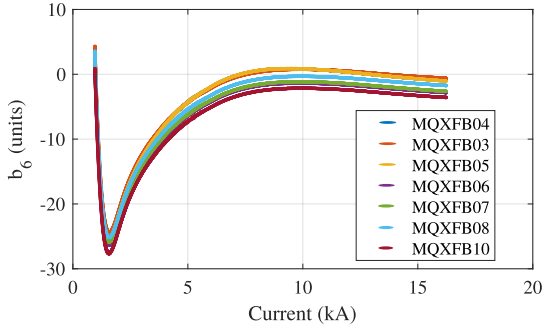


Figure 4: b_6 as a function of current during machine cycles. The steep change at low field is due to the superconductor magnetization (persistent currents).

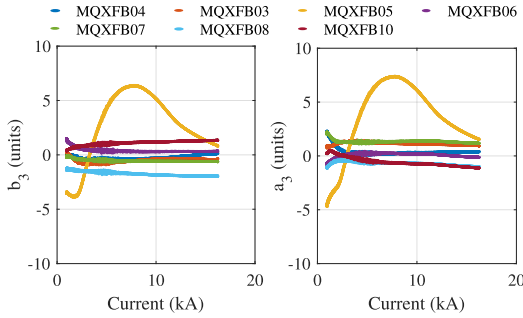


Figure 5: b_3 and a_3 as functions of current during machine-cycle ramps. The change observed in MQXFB05 is the effect of magnetic shims.

WARM-TO-COLD EXTRAPOLATION

Sorting and matching MQXF magnets within circuit (Q2A and Q2B) is an effective way to reduce β -beating (through pair calibration) and optimize beam calibration [10]. For an effective magnet sorting, it is important to estimate the transfer function at nominal operating conditions as early as possible [11]. Since the ambient temperature measurements are available several months before the cryogenic measurements, a warm-to-cold extrapolation model has been developed.

The extrapolation model separates the effects on the cross-section (TF_{ctr}) from the effects on the magnetic length (L_m), and accounts for thermal contraction, iron saturation, residual magnetization, and the effect of magnetic shimming. The integrated transfer function at nominal current can be written as

$$TF_{int}^{nom} = TF_{ctr}^{nom} L_m^{nom},$$

where

$$L_m^{nom} = L_m^{warm} cf_L + sat_L,$$

and

$$TF_{ctr}^{nom} = TF_{ctr}^{warm} + rm_G + cf_G - sat_G + sat_S.$$

Here, cf_L is the contraction factor for the magnetic length, sat_L is the contribution of iron saturation to the magnetic length, rm_G is the residual magnetization contribution, cf_G is the contribution of thermal contraction to the central field, sat_G is the contribution of iron saturation to the central field, and sat_S is the contribution of magnetic shimming.

The coefficients associated with magnetic shimming were derived from magnetic simulations, while all other coefficients were obtained from calibration against the prototype magnets and the first three series units. The use of calibration data from a limited number of early-production magnets is the main source of uncertainty in the extrapolation model.

Table 4: Extrapolation Coefficients for TF Prediction

Coefficient	Value	Units
cf_L	0.9978	–
sat_L	0.0159	m
rm_G	0.1170	$T m^{-1} kA^{-1}$
cf_G	0.0135	$T m^{-1} kA^{-1}$
sat_G	0.8140	$T m^{-1} kA^{-1}$
sat_S	0.003 * N. blades	$T m^{-1} kA^{-1}$

Table 5: Measured and Extrapolated TF at Nominal

Magnet	TF meas. [T/kA]	TF extr. [T/kA]	Error [units]
MQXFB03	58.571	58.542	-5
MQXFB04	58.654	58.568	-15
MQXFB05	58.700	58.643	-10
MQXFB06	58.523	58.495	-5
MQXFB07	58.563	58.542	-4
MQXFB08	58.594	58.568	-4
MQXFB10	58.554	58.487	-11

The comparison between measured and extrapolated transfer functions is reported in Table 5. It shows that the extrapolation error has a systematic component of -7 units, and a random component of 5 units at 1-sigma. This level of accuracy is sufficient for magnet sorting given the spread of the magnet production in the range of 36 units, see Table 2.

CONCLUSIONS

The magnetic measurement program of the MQXFB quadrupoles for the HL-LHC has provided a complete characterization of the field quality during production. Ambient temperature measurements allow early detection of geometric errors, while cold measurements at 1.9 K quantify the field quality under nominal operating conditions.

The measured transfer function spread is within 36 units, and the field harmonics are within the expected range. Magnetic shimming has proven to be effective for correcting selected low-order multipoles. The warm-to-cold extrapolation predicts the nominal transfer function with an accuracy compatible with 5×10^{-4} , enabling reliable sorting before the final cold test of all magnets.

ACKNOWLEDGMENT

We gratefully acknowledge the work of the teams at CERN for both manufacturing and testing and the regular, open, and fruitful exchange with colleagues within the HL-LHC community.

REFERENCES

- [1] O. Aberle *et al.*, *High-Luminosity Large Hadron Collider (HL-LHC): Technical design report*. Geneva: CERN, 2020. doi:10.23731/CYRM-2020-0010
- [2] A. Milanese *et al.*, “Status of MQXFB quadrupole magnets for HL-LHC”, in *Proc. IPAC'23*, Venice, Italy, pp. 3704–3707, Sep. 2023. doi:10.18429/JACoW-IPAC2023-WEPM060
- [3] S. I. Bermudez *et al.*, “Status and challenges in the mqxfb nb3sn quadrupoles for the hl-lhc”, *IEEE Trans. Appl. Supercond.*, vol. 35, no. 5, pp. 1–7, 2025. doi:10.1109/TASC.2025.3530911
- [4] L. Fiscarelli *et al.*, “Measurement of integrated gradient and field quality on the first Q2 magnets for HL-LHC”, in *Proc. IPAC'24*, Nashville, TN, USA, pp. 2847–2850, Jul. 2024. doi:10.18429/JACoW-IPAC2024-WEPS64
- [5] P. Rogacki, L. Fiscarelli, S. Russenschuck, and K. Hameyer, “A rotating-coil scanner for the precise magnetic characterization of superconducting accelerator magnets at ambient temperature”, *IEEE Trans. Magn.*, vol. 57, no. 2, pp. 1–5, 2021. doi:10.1109/TMAG.2020.3005722
- [6] S. Russenschuck, “Theory of the coil magnetometer”, in *Field Simulation for Accelerator Magnets*. John Wiley & Sons, Ltd, 2025, pp. 357–413. doi:10.1002/9783527839599.ch10
- [7] S. Russenschuck, “Stretched-wire field measurements”, in *Field Simulation for Accelerator Magnets*. John Wiley & Sons, Ltd, 2025, pp. 415–467. doi:10.1002/9783527839599.ch11
- [8] M. Pentella, S. I. Bermudez, C. Petrone, H. Prin, S. Russenschuck, and E. Todesco, “Field-axis measurement of an ac-powered magnet by a single stretched wire”, *Meas.: Sens.*, vol. 38, p. 101429, 2025. doi:10.1016/j.measen.2024.101429
- [9] S. Izquierdo Bermudez *et al.*, “Magnetic analysis of the mqxf quadrupole for the high-luminosity lhc”, *IEEE Trans. Appl. Supercond.*, vol. 29, no. 5, pp. 1–5, 2019. doi:10.1109/TASC.2019.2897848
- [10] A. Fornara, G. Sterbini, and M. Giovannozzi, “Current classification strategies based on the transfer function and field quality of the new superconducting magnets in the HL-LHC”, presented at IPAC'26, Deauville, France, May 2026, paper WEP5068, this conference.
- [11] A. Fornara, G. Sterbini, L. Fiscarelli, M. Giovannozzi, and S. I. Bermudez, “HL-LHC magnets field quality: Current situation, strategies and mitigation measures”, presented at IPAC'26, Deauville, France, May 2026, paper WEP5069, this conference.